HYDROLOGICAL PROCESSES
*Hydrol. Process.* (2016)
Published online in Wiley Online Library
(wileyonlinelibrary.com) DOI: 10.1002/hyp.10787

# T-NET, a dynamic model for simulating daily stream temperature at the regional scale based on a network topology

A. Beaufort,[1]* F. Curie,[1] F. Moatar,[1] A. Ducharne,[2] E. Melin[3] and D. Thiery[4]

[1] *EA 6293 GéHCO Géo-Hydrosystèmes Continentaux, Université François-Rabelais de Tours, Parc de Grandmont, Tours 37200, France*
[2] *UMR METIS, UPMC, Case 105, T56-46 4ème étage, 4, place Jussieu75252Paris Cedex 05, France*
[3] *EA 4022, LIFO 4, Université d'Orléans (France), Rue Léonard de VinciBP 6759 45067Orleans Cedex 2, France*
[4] *Bureau de Recherches Géologiques et Minières (BRGM), BP 6009 45060Orléans Cedex 2, France*

## Abstract:

Currently, the distribution areas of aquatic species are studied by using air temperature as a proxy of water temperature, which is not available at a regional scale. To simulate water temperature at a regional scale, a physically based model using the equilibrium temperature concept and including upstream-downstream propagation of the thermal signal is proposed. This model, called Temperature-NETwork (T-NET), is based on a hydrographical network topology and was tested at the Loire basin scale ($10^5\,km^2$). The T-NET model obtained a mean root mean square error of 1.6 °C at a daily time step on the basis of 128 water temperature stations (2008–2012). The model obtained excellent performance at stations located on small and medium rivers (distance from headwater <100 km) that are strongly influenced by headwater conditions (median root mean square error of 1.8 °C). The shading factor and the headwater temperature were the most important variables on the mean simulated temperature, while the river discharge influenced the daily temperature variation and diurnal amplitude. The T-NET model simulates specific events, such as temperature of the Loire during the floods of June 1992 and the thermal regime response of streams during the heatwave of August 2003, much more efficiently than a simple point-scale heat balance model. The T-NET model is very consistent at a regional scale and could easily be transposed to changing forcing conditions and to other catchments.


KEY WORDS thermal model; daily stream temperature; dynamic regime; equilibrium temperature; Loire basin; regional scale

*Received 9 July 2015; Accepted 5 January 2016*

## INTRODUCTION

Current ecological research focuses on the impact of climate change on the distribution area of fish species (Buisson and Grenouillet, 2009; Tisseuil *et al.,* 2012; Domisch *et al.,* 2013). These studies are carried out at a regional scale (>50 000 $km^2$) and use air temperature as a proxy of stream temperature because water temperature records are not available at all sampling sites (Buisson *et al.,* 2008; Sharma *et al.,* 2007; Lassalle and Rochard, 2009). However, air temperature may be a poor surrogate for stream temperature, particularly in headwater reaches (Caissie, 2006) and for rivers fed by groundwater (O'Driscoll and DeWalle, 2006). In that sense, working on the distribution area of fish species with simulated stream temperature could allow more accurate predictions from ecological models. This may be conducted at different scales, ranging from large rivers to small streams.

Several physically based models accounting for the heat balance of the river have been used successfully to simulate stream temperature and to develop water quality plans (Chapra *et al.,* 2008; Boyd and Kasper, 2003; Cole and Wells, 2002). The physically based modelling approach has the advantage of being very detailed, as it can take into account all relevant heat fluxes at both the water surface and sediment water interface, and it is therefore particularly suitable for climate change impact studies (Bustillo *et al.,* 2014). However, one-dimensional or two-dimensional deterministic thermal models are generally restricted to single segment rivers (Carrivick *et al.,* 2012; Ouellet *et al.,* 2014) or to small catchments (Cox and Bolte, 2007; Loinaz *et al.,* 2013) and are not applied at a regional scale (>$10^5\,km^2$). This can be explained by the amount of input data that are required but are rarely available at this scale and also by the considerable amount of computing time required by this type of model. To our knowledge, the RBM model (Yearsley, 2009, 2012), using a semi-Lagrangian numerical scheme to solve the one-dimensional, time-

*Correspondence to: A. Beaufort, Université François-Rabelais de Tours, EA 6293 GéHCO Géo-Hydrosystèmes Continentaux, Parc de Grandmont 37200 Tours, France
E-mail: aurelien.beaufort@hotmail.fr
Contract/grant sponsor: Agency of Loire Bretagne (AELB).

dependent equations for thermal energy balance in advective river systems, is the only thermal model that has been applied at a regional scale (35 000 km$^2$). It has been used to study the impact of climate changes on large rivers (catchment area between $4 \times 10^4$ and $3 \times 10^6$ km$^2$; van Vliet *et al.,* 2012) and to assess the impact of anthropogenic effects on temperature on small catchments (31 km$^2$; Sun *et al.,* 2014).

River temperature controls are multivariate and nested at regional, sub-basin, reach or site-specific scale (Hannah and Garner, 2015). At regional scale, climate (solar radiation and air temperature) drives the thermal regime of rivers, but at smaller scales, the riparian shading (Moore *et al.,* 2005) and groundwater inputs could strongly influence the local water temperature (Garner *et al.,* 2014). However, most of the previous studies have been restricted to the sub-basin scale or limited to studding the influence of site-specific factors at a local scale, and there is a lack of research on spatial and temporal variability and controls on river temperature at a regional scale (Hannah and Garner, 2015).

A previous study (Beaufort *et al.,* 2015) on the Loire basin aimed at simulating the thermal regime of streams using a simplified 0D thermal model discretized by Strahler order and including all relevant heat fluxes at both the water surface and sediment/water interface as proposed by Herb and Stefan (2011); it highlighted the difficulty of adequately simulating temperatures on smaller order that are very dependent on their upstream conditions. The thermal dynamics of upstream rivers are similar to groundwater temperature because the time of exposure is not sufficient to equilibrate the water temperature with the atmosphere (Kelleher *et al.,* 2012). The relation between the thermal regime of rivers and climate conditions becomes stronger when the distance from headwater increases (Garner *et al.,* 2013). However, this 0D thermal model ignores advective processes that determine the upstream–downstream propagation of thermal signals. Taking these advective processes into account was expected to be a major factor to account for the thermal regime of small and medium streams (first to fifth Strahler order).

In this study, we tested an approach based on the equilibrium temperature concept (Edinger *et al.,* 1968, 1974), which includes the upstream–downstream propagation of the thermal signal and offers an appealing way of overcoming these previous difficulties, because: (i) the equilibrium temperature ($T_e$) and the thermal exchange coefficient ($K_e$) are exclusively defined by climate forcing conditions and groundwater inflow and thus constitute the only common denominators for studying the thermal regime of distinct rivers with contrasted characteristics and (ii) it is possible to simulate the rate at which the river temperature reaches equilibrium. In line with Mohseni and Stefan (1999), it is possible to simulate the upstream–downstream propagation of the thermal signals by rearranging the fundamental equation underlying the equilibrium temperature concept and considering the flow velocity as known.

The main objective of this work was to develop a new dynamic model based on a network topology (T-NET model) at a regional scale. The capacity of this new model to simulate the daily water temperature in relation to the distance from the headwater was assessed over a 4-year period (2008 to 2012) at 128 stations. The efficiency of the T-NET model was compared with that of the 0D model described by Beaufort *et al.* (2015) based on the same validation set. Particular attention was paid to the performance of stations according to the distance from their headwater by differentiating between stations located on small (<30 km from headwater), medium (between 30 and 100 km) and large rivers (>100 km from headwater). These distances were determined on the basis of work by Beaufort *et al.* (2015), who found that the 0D thermal model had difficulty simulating water temperature on small and medium rivers [mean daily root mean square error (RMSE) over summer >2.0 °C], while simulations were excellent for large rivers (mean daily RMSE over summer <1.5 °C). Finally, we compared the ability of the T-NET model and the 0D model tested by Beaufort *et al.* (2015) to simulate temperatures during exceptional events: (i) the summer flood of 1992 and the winter flood of 2003 in the Middle Loire and (ii) the heat wave of summer 2003 and the cold summer of 2002. The final aim was to identify the most important input data on temperature calculations by carrying out a sensitivity analysis.

### *Study site*

The Loire basin comprises a hydrographical network of 88 000 km and drains a catchment area of 117 000 km$^2$. It is characterized by varying climate between the upstream and the downstream (annual rainfall between 600 and 1300 mm per year and annual air temperature between 6 and 12.5 °C); landform (10% of the basin area >800 m; mean altitude = 300 m); and lithology (metamorphic, magmatic and sedimentary rocks). Streams located in the central part of the basin, mainly composed of sedimentary rocks, benefit more from groundwater supplies.

Water temperature ($T_w$) was monitored at 128 stations between 2008 and 2012 (see Section on Validation of the T-NET Model). The highest mean annual temperatures were observed on large rivers such as the Loire (Strahler order 8) and its main tributaries, where mean annual temperatures ranged between 14 and 16 °C between 2008 and 2012 (Figure 1a). Colder temperatures (<9 °C) were observed in the upstream reaches of the Loire where the

 

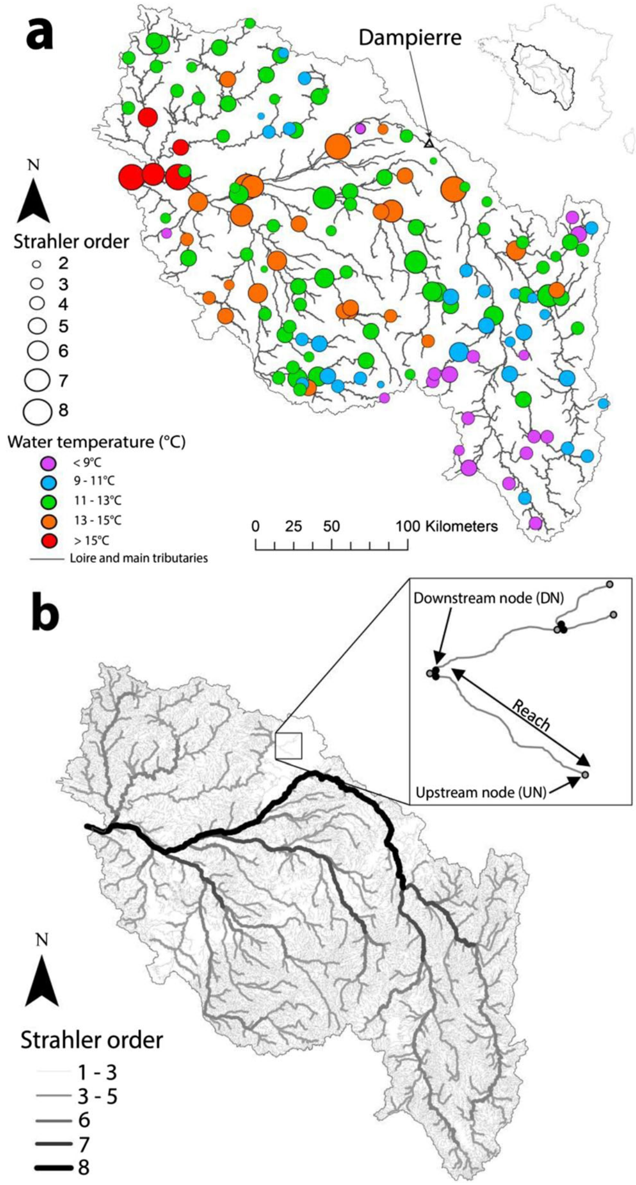


Figure 1. Loire Basin and data presentation: (a) 128 stream temperature monitoring stations and 368 subwatersheds used to simulate daily flows and (b) hydrographical network (52 200 reaches) used to simulate the stream temperature

altitude is above 1000 m. The annual water temperature at stations located on small streams (51 stations at < 30 km from headwaters) did not exceed 13 °C (Figure 1a).

## MODEL AND DATASETS

### *Principle of the T-NET model*

The principle of the T-NET model consists of calculating changes in water temperature along the stream network based on a hydrographical network topology, taking spatial and temporal dimensions into account (Figure 1b). This calculation was carried out in three steps. The first involved simulating the equilibrium temperature ($T_e$) by resolution of the heat budget. In the second step, the longitudinal variation of the water temperature was simulated between the upstream node (UN) and the downstream node (DN) of each reach, taking into account the speed at which the water temperature converged with the equilibrium temperature (Figure 2; Equation 3). The third step occurred at the confluence of two reaches, where the thermal signal from the two reaches was mixed with respect to their discharge in order to determine the temperature at the UN of the downstream reach (Figure 2; Equation 4). These three steps enabled us to calculate the water temperature in each of the 52 200 reaches of the hydrological network located in the Loire basin. The mean length of the 52 200 reaches

 

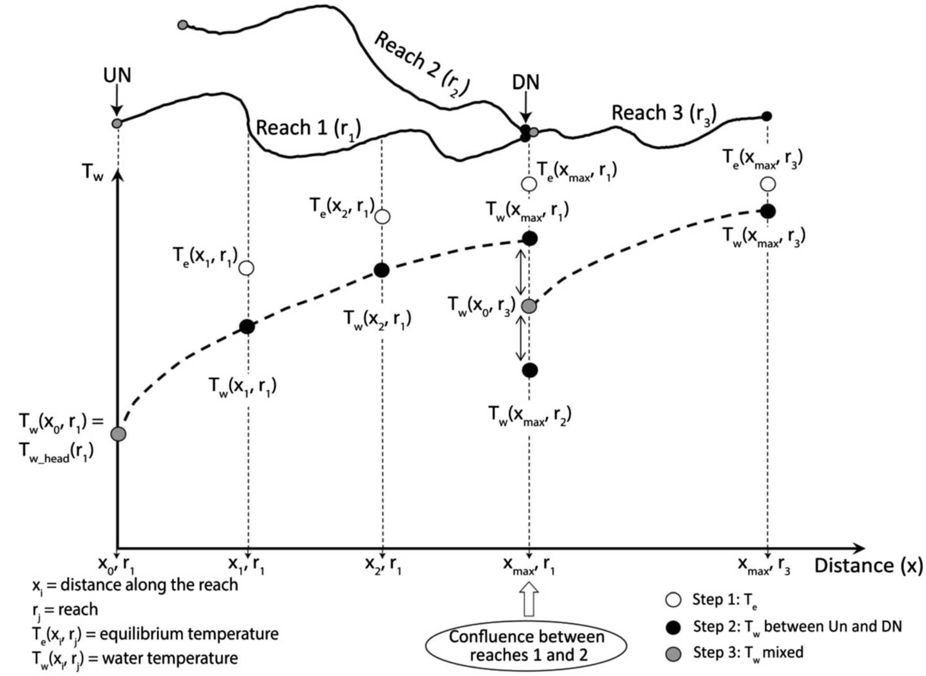


Figure 2. Pattern of upstream–downstream propagation of thermal signal at a given time $t$

is 1.7 km. Because of the small transfer time of flows through each reach (less than a day) causing routing problems, all temperature simulations were conducted at an hourly time step (Figure 1b) and were then averaged per day for the validation and the exploitation of the T-NET model.

- Computation of the equilibrium temperature

Assuming steady-state conditions, Equation 1 describes the rate of change of mean temperature with distance due to mean surface heat transfer and groundwater inputs:

$$\frac{\partial T_w}{\partial \chi} = \frac{K_e B}{\rho_w C p_w Q}(T_e - T_w) \quad (1)$$

$$\sum_i H_i = H_{ns} + H_{la} - H_{lw} + H_c - H_e + H_g \quad (2)$$

where $T_w$ is the water temperature [°C], $T_e$ is the equilibrium temperature [°C], $K_e$ is the heat exchange coefficient (J s$^{-1}$ m$^{-2}$ K$^{-1}$), $x$ is the distance (m), $\rho_w$ is the density of water (kg m$^{-3}$), $Cp_w$ is the specific heat of water (J kg$^{-1}$ K$^{-1}$), $Q$ is the river discharge (m$^3$ s$^{-1}$) and $B$ is the river width (m) and $\sum H_\mathrm{i}$ is the net heat flux (J s$^{-1}$ m$^{-2}$). The equilibrium temperature ($T_e$) is defined as the water temperature ($T_w$) at which the total heat flux ($\sum H_\mathrm{i}$) at the limit of the water body is 0 (Equation 2). Six heat fluxes (W m$^{-2}$) were included (Table I): $H_{ns}$ is the net solar radiation, $H_{la}$ is the atmospheric long-wave radiation, $H_{lw}$ is the long-wave radiation emitted from the water surface, $H_\mathrm{e}$ is the evaporative heat flux, $H_c$ is the convective heat flux exchanged with the atmosphere and $H_g$ is the groundwater heat inflow. In line with Edinger *et al.* (1968), the heat exchange coefficient $K_e$ was computed with a theoretical formulation corresponding to the sum of derivatives of heat fluxes with respect to water temperature (Bustillo *et al.,* 2014; Beaufort *et al.,* 2015), which is thus easily applicable at a regional scale.

$$K_e(t) = 4\varepsilon\sigma(T_w(t) + 273.15)^3 + f(w) \left(0.62 + 6.11.\frac{17.27\times 237.3}{(237.3 + T_w(t))^2} \times \exp\left[\frac{17.27\times T_w(t)}{237.3+T_w(t)}\right]\right) + \rho_w C p_w \frac{Q_g(t)}{A} \quad (3)$$

where $f(w)$ is the wind function, taken from Brutsaert and Stricker (1979) (Table I) and $Q_g/A$ defines the seepage flux (m s$^{-1}$). $T_e$ and $K_e$ were computed every hour for each reach, taking into account meteorological variables and groundwater inputs (Figure 2; step 1).

- Upstream–downstream propagation of the thermal signal

The headwater temperature ($T_{\mathrm{w\_head}}$) of the upstream boundary of the network (reach with a Strahler order 1) was fixed as the groundwater temperature approximated by adding 1 °C to the moving average of the air temperature over 365 days preceding the observation (see Section on Datasets). The travel time (*TT*) of the water between the UN and the DN of a reach was

 

Table I. Formulations and parameters used to determine heat fluxes occurring at the water/air and water/sediment interface (Bustillo et al., 2014; Sridhar et al., 2004; Brutsaert and Stricker, 1979)

| Heat flux ($W\,m^{-2}$) | Formulations | Parameters | Assumptions |
|---|---|---|---|
| Net solar radiation ($H_{ns}$) | $H_{ns} = (1 - Alb) \cdot Rg \cdot (1 - SF)$ | Alb: surface water albedo<br>Rg: global radiation ($W\,m^{-2}$)<br>SF: shading factor | $Alb = 0.06$ |
| Long-wave radiation ($H_{la}$) | $H_{la} = \varepsilon_a \cdot \sigma \cdot (T_a + 273.15)^4 \times \left(1 + 0.22 \cdot Cld^{2.75}\right)$ | $\varepsilon_a$: clear-sky atm. emissivity<br>$\sigma$: Boltzmann constant<br>$Ta$: air temperature (°C)<br>$Cld$: cloud cover fraction | $\varepsilon_a$ = constant<br>$\sigma = 5.67 \times 10^{-8}\ J\,s^{-1}\,m^{-2}\,K^{-4}$ |
| Long-wave emitted radiation ($H_{lw}$) | $H_{lw} = \varepsilon_w \cdot \sigma \cdot (T_w + 273.15)^4$ | $\varepsilon_w$: Water emissivity<br>$T_w$: Water temperature (°C) | $\varepsilon_w = 0.97\sigma = 5.67 \times 10^{-8}\ J\,s^{-1}\,m^{-2}\,K^{-4}$ |
| Convection ($H_c$) | $H_c = B \cdot f(w) \cdot (T_a - T_w)$ | $B$: Bowen's coefficient<br>$f(w) = aw + b$ : wind function<br>$w$: wind speed at 2 m ($m\,s^{-1}$) | $a = 4$ ($W\,s\,m^{-3}\,mb^{-1}$)<br>$b = 7.4$ ($W\,m^{-2}\,mb^{-1}$)<br>$B = 0.62\ mb\,K^{-1}$ |
| Evaporation ($H_e$) | $H_e = f(w) \cdot (e_s - e_a)$ | $e_a$: water vapour pressure in air (mb)<br>$e_s$: saturation vapour pressure for$T_w$ (mb) | Magnus–Tetens approximation:<br>$e_s = 6.11 \cdot \exp\left(\frac{17.27 \cdot T_w}{237.3 + T_w}\right)$ |
| Streambed inputs ($H_g$) | $H_g = \rho_w Cp_w \frac{Q_G}{A}\left(T_g - T_w\right)$ | $T_g$: groundwater temperature (°C)<br>$\rho_w$: density of water ($kg\,m^{-3}$)<br>$Cp_w$: specific heat capacity ($J\,kg^{-1}\,°K^{-1}$)<br>$Q_g$: groundwater flow ($m^3\,s^{-1}$)<br>$A$: exchange area betweengroundwater and river ($m^2$) | |

determined by taking into account the flow velocity ($U$) and the reach length ($L$).

$$TT\left(r_j\right) = \frac{L\left(r_j\right)}{U\left(r_j\right)} \quad (4)$$

where $L$ is reach length (m), $U$ is flow velocity ($m\,s^{-1}$), $TT$ is travel time (h) and $r_j$ is the reach where the water temperature was calculated ($j = 1$ to 52 200). Meteorological variables have an hourly temporal resolution, and discharge simulations are at a daily time step and considered constant over 24 h. If the $TT$ of a reach $j$ was less than 1 h, meteorological variables and hydrological forcing (flow velocity and depth) remained constant. In that case, the temperature at the DN could be directly calculated with Equation 4 where Equation 1 was solved for $T_w(x_i, r_j)$ in order to determine the longitudinal variation in the mean stream temperature after a travel along a length scale $x_i$:

$$T_w\left(\chi_{i+1} r_j\right) = T_e\left(\chi_{i+1},, r_j\right) + \left[T_w\left(\chi_{i,} r_j\right) - T_e\left(\chi_{i+1,} r_j\right)\right] \quad (5)$$
$$.\exp\left[\frac{-B\left(r_j\right).K_e\left(\chi_{i+1}, r_j\right)}{\rho_w Cp_w Q\left(r_j\right)} \Delta\chi\right]$$

where $x_i$ is the location on the reach length $r_j$ (m) and $\Delta x$ ($\Delta x = x_{i+1} - x_i$) is the length of the space increment (m). If $TT$ was more than 1 h, steady-state conditions did not exist and the water temperature changed every hour in relation to meteorological variables. In that case, the reach was discretized into several sections, taking into account $TT$ and the reach length (Equation 4). Each section ($\Delta x$) in the reach had the same length and corresponded to the distance travelled by the water in 1 h, corresponding to the temporal resolution of meteorological variables. This allowed changes in water temperature to be calculated every hour by a succession of 'short-term' simulations where meteorological and hydrological features were constants (Figure 2; step 2). In order to determine the water temperature at the DN at time $t$, the temperature at the UN was taken at time $t = t - TT$, followed by a succession of independent simulations from the UN to the final increment ($x_{\max}$) and computed by Equation 5. The heat budget was determined at each increment, and the water temperature $T_w(x_i, r_j)$ was recalculated. The temperature calculated at the final increment, $T_w(x_{max}, r_j)$, corresponded to the temperature of the UN propagated along the reach during TT.

At the confluence of two reaches (reaches 1 and 2; Figure 2; step 3), the thermal signal from the two reaches was mixed with respect to their discharge in order to determine the temperature at the UN of the downstream reach (black dots; Figure 2):

$$T_w\left(\chi_0, r_{j+2}\right) = T_w\left(\chi_{\max}, r_j\right) \times \left(\frac{Q\left(\chi_{\max}, r_j\right)}{Q\left(\chi_0,, r_{j+2}\right)}\right) + T_w\left(\chi_{\max},, r_{j+1}\right) \times \left(\frac{Q\left(\chi_{\max},, r_{j+1}\right)}{Q\left(\chi_0,, r_{j+2}\right)}\right) \quad (6)$$

where $Q(x_{\max}, r_j)$ is the discharge of the headreach $r_j$ ($m^3\,s^{-1}$), $Q(x_{\max}, r_{j+1})$ is the discharge of the headreach

 

$r_{j+1}$ ($m^3 s^{-1}$) and $Q(x_0,r_{j+2})$ is the discharge upstream of the reach $r_{j+2}$ ($m^3 s^{-1}$). It should be noted that the mixing of the thermal signal between two streams is conducted with a simplified method in which only taking into account of the discharge and the time of the well-mixed volume of water is considered instantaneous (Equation 6). It was thus possible to calculate changes in water temperature along the reach $r_{j+2}$ $T_w(x_0,r_{j+2})$ using Equations 4, 5 and 6.

*Datasets*

*Meteorological forcing variables*. Meteorological variables were used to calculate the equilibrium temperature ($T_e$), the heat exchange coefficient ($K_e$) and the groundwater temperature ($T_g$). Hourly data of meteorological variables were taken from the SAFRAN atmospheric reanalysis (Quintana-Segui *et al.*, 2008; Vidal *et al.,* 2010), which was produced by Meteo-France with an 8-km resolution for the period 1970–2007 for the following near-surface parameters: air temperature (°C), specific humidity ($g\,kg^{-1}$), wind velocity ($m\,s^{-1}$), global radiation ($W\,m^{-2}$) and atmospheric radiation ($W\,m^{-2}$). Meteorological variables were incorporated into each reach, depending on its location in the SAFRAN grid, and weighted taking into account the ratio between the length of the reach within a grid cell and the total reach length (Figure 3).

*Hydrological forcing variables*. The mean discharge values ($Q$) and groundwater flows ($Q_g$) ($m^3 s^{-1}$) were simulated by the semi-distributed hydrological model EROS (Thiéry, 1988; Thiéry and Moutzopoulos, 1995) at the outlet of 368 subwatersheds (ranges between 40 and 1600 $km^2$; mean drainage area = 300 $km^2$), designed to be as homogeneous as possible with respect to land use and geology. These values were then redistributed into the rivers located within each subwatershed according to their own drainage area in order to determine discharges in any reach of the network (Figure 3). To test the performance of the hydrological model at medium and low flows, Nash criteria were calculated on the squared differences between observed and simulated discharges (C1), on the square roots of discharges (C2) and on the logarithms of discharges (C3), providing a better assessment of high flow period (C1), average flow period (C2) and low-flow period (C3). Performance was good at the 352 validation stations with a minimum of 10 years of continuous measurement between 1984 and 2012: 92% of stations had a C1 criterion higher than 0.7, and all the C2 and C3 criteria were higher than 0.6. In other words, all the rivers

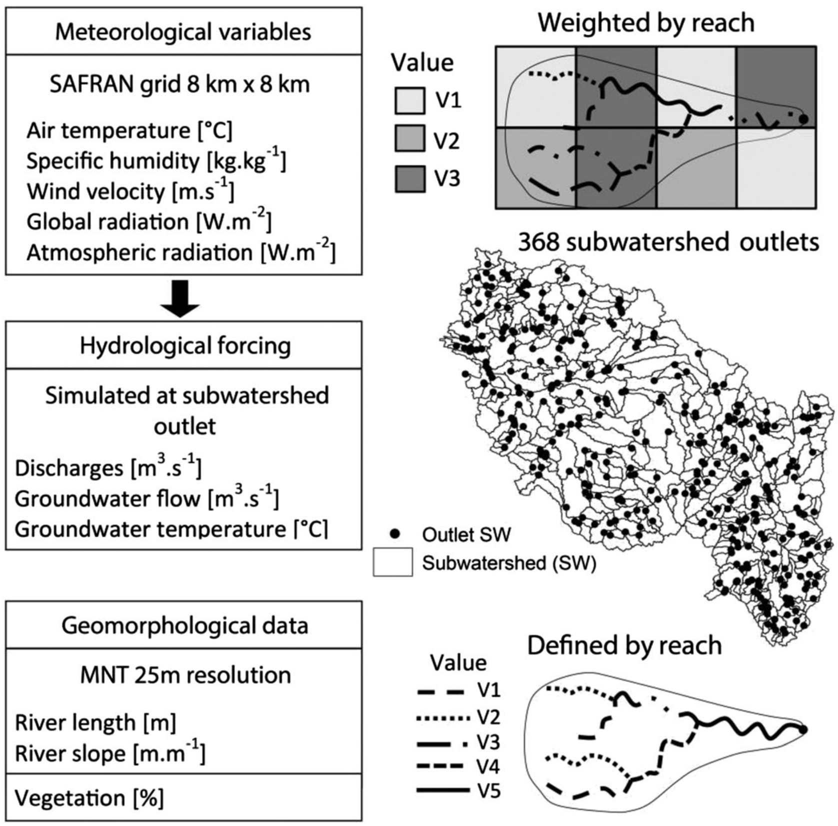


Figure 3. Input data and discretization into the T-NET model

with the same order in the same subwatershed had a similar discharge. Only five subwatersheds had a Nash criterion (C1, C2 and C3) less than 0.6, and no water temperature measurement station was located inside that subwatersheds poorly simulated. The surface discharge ($Q$) and groundwater flows ($Q_g$) are considered constant over a day (24 h) for the calculation of the hourly temperature (Equations 1, 3 and 4).

Only 31 500 one-off measures of groundwater temperature in unconfined aquifers were available at 890 measurement stations between 1976 and 2012. In order to determine the groundwater temperature across the entire basin, $T_g$ was estimated by adding 1 °C to the moving average of the air temperature over 365 days preceding the observation, in accordance with Todd (1980). The groundwater temperature was validated at 890 stations, the median RMSE calculated for the 31 500 measures was 1.6 °C (ranging between 2.5 and 0.8 °C), and the coefficient of determination ($R^2$) is 0.7 and higher than 0.6 at 70% of stations. The median bias was 0.4 °C, and 60% of biases were between −0.5 and 0.5 °C. The performance is globally similar over the year, and no seasonality in bias has been identified. This simple method of determining the groundwater temperature seems adequate for a large number of rivers.

*Geomorphological and vegetation data*. The main characteristics (length and slope) of the drainage network were extracted from the CARTHAGE® (Thematic cartography of water agencies and French ministry of environment) database and the BD ALTI® 25-m resolution digital terrain model dataset for each reach (Figure 3). The reach width ($B(r_j)$) and depth ($D(r_j)$) were determined daily using the ESTIMKART application, which takes into account the reach slope and the mean and daily flows of the reaches (Lamouroux *et al.,* 2010), assuming a rectangular cross-section.

$$B(t) = a_d \overline{Q}^{b_d} \left[ \frac{Q(t)}{\overline{Q}} \right]^b \quad (7)$$

$$D(t) = c_d \overline{Q}^{f_d} \left[ \frac{Q(t)}{\overline{Q}} \right]^f \quad (8)$$

where $\overline{Q}$ is the mean flow ($m^3 s^{-1}$), $Q$ is the daily flow ($m^3 s^{-1}$) and b, f, $a_d$, $b_d$, $C_d$, $f_d$ are coefficients and exponents, depending on river slope, watershed area and Strahler order Lamouroux *et al.* (2010). Reach width, length ($L(r_j)$) and depth were considered constant over 24 h and were used to determine the flow velocity ($U(r_j)$) and the exchange area ($A(r_j) = D(r_j)*B(r_j)*L(r_j)$) between the reach and the groundwater for the calculation of the groundwater heat flux $H_g$. Reach width was also included in the water temperature equation (Equation 2). The reach width and depth were compared with one-off measurements at 183 stations on streams with drainage areas ranging between 5 and 15 000 km$^2$. Geomorphological values were close to observations, and the mean RMSE obtained on the basis of these 183 measures for reach width and depth was respectively 4 m and 0.2 m.

A shading factor (SF), corresponding to a coefficient of reduction of the overall incident radiation ($H_{ns}$), was estimated from the database of Valette *et al.* (2012), which gives the averaged vegetation cover (%) determined by remote sensing on both sides of reaches with a buffer of 10 m for each reach. The vegetation cover was averaged for each reach and weighted linearly by a coefficient determined by calibration, linked to the Strahler order, ranging from 1 for a Strahler order 1 to 0 for a Strahler order 8, to account for the influence of reach width on shading area (Beaufort *et al.,* 2015).

*Validation of the T-NET model*. There are 128 hourly monitoring stations managed by the National Office for Water and Aquatic Environments available between July 2008 and December 2012. Of these, 47 stations recorded summer temperatures (July–August) in 2002 and 2003. Summer 2003 was marked by a severe drought (1 in 50 years) and a hot spell (Moatar and Gailhard, 2006), with an increase of 3.2 °C in the mean summer air temperature ($T_a$) compared with the 1974–2006 summer mean. Stations are distributed across the whole basin, although there are fewer in the southeastern area (Figure 1a). Validation stations cover a wide range of stream sizes with drainage areas ranging from 3 to 110 000 km$^2$ (Figure 1a). Most sampling occurs in medium-sized rivers, with 39 stations on rivers with drainage areas of between 150 and 500 km$^2$ (Figure 1a). The electricity-generating authority (EDF) provided the water temperature data for 1992 and 2003 at the Dampierre station, located 580 km downstream of the Loire's source.

## RESULTS AND DISCUSSION

### *Performance of simulations*

The T-NET model faithfully represents the daily water temperature observed at 128 measurement stations between 2008 and 2012 with a mean RMSE of 1.6 °C, and 30% of stations had an RMSE less than 1.5 °C (Figure 4a). Mean annual biases were close to 0, with about 60% of stations having an annual bias of between −0.5 and 0.5 °C (Figure 4b), and standard deviations of errors were lower than 1 °C for 55% of stations. Nash criteria were calculated on the square roots of temperatures, and 71% of stations obtained a Nash criteria higher than 0.8 against only 6% of stations with a Nash criteria less than 0.4 (Figure 4c).

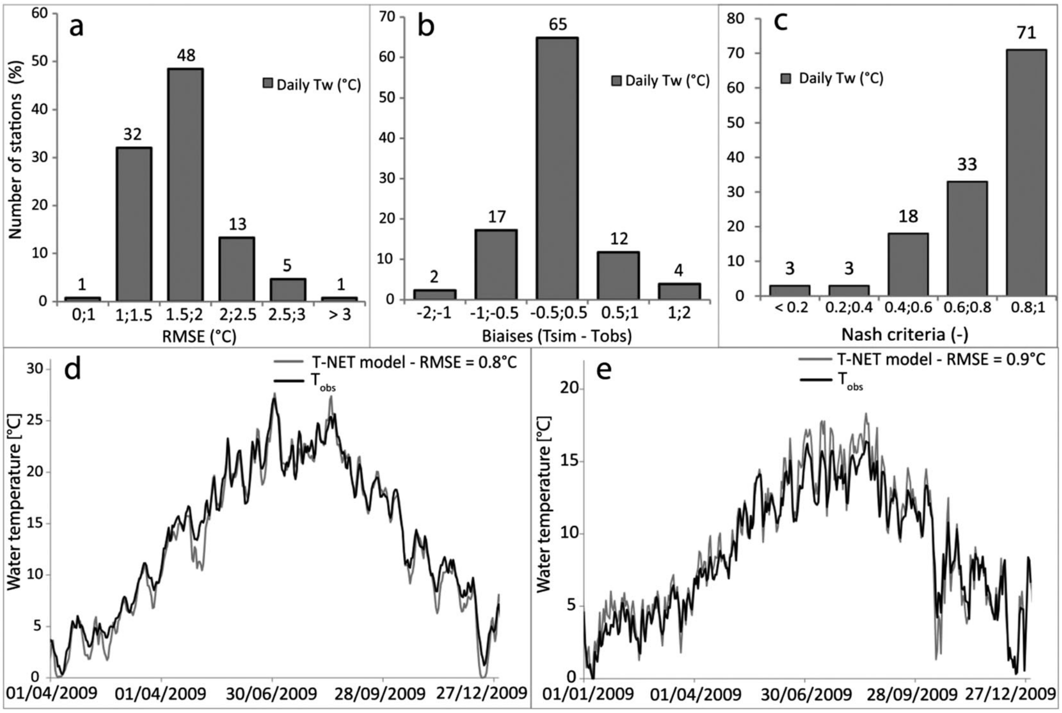


Figure 4. Distribution of mean multi-annual (a) root mean square errors (b) biases and (c) Nash criterion, with the T-NET model validated at an hourly and daily time step. Daily observed and simulated water temperatures at two stations in 2009: (d) on the Loire River at Muisdes-sur-loire (drainage area = 38,300 km$^2$) and (e) on the Vincou River at Thouron (drainage area = 81 km$^2$)

Two examples of daily simulations are displayed for two stations: one on a large river and the other on a small river (Figure 4d and e). The T-NET model produced good daily simulations where the mean daily RMSE over the year could be less than 1 °C (Figure 4d and e). For small and medium rivers (Figure 5a and b), simulated summer temperatures were overestimated by 0.8 °C on average. Monthly biases were negative in spring (−0.5 °C) and autumn (−0.5 °C) and positive between January and March (0.7 °C) for small rivers (Figure 5a). The model underestimated the water temperature of medium rivers by 0.7 °C on average in November. Monthly biases were close to 0 for large rivers (distance from headwater >100 km) during the year, but with a slight underestimation (0.3 °C) in autumn and winter (Figure 5c). The daily RMSE average over each month has the same behaviour throughout the year whatever the river size with a higher RMSE in summer (RMSE = 1.8 °C) and in winter (RMSE = 1.7 °C) and better performance in spring and autumn (RMSE = 1.5 °C) (Figure 5d–f). However, the performance during winter was poorer for small reaches with an RMSE higher than 2 °C (Figure 5d). The standard deviation was regular over the year and equal to 1 °C on average whatever the river size.

*Comparison of the T-NET and 0D models*

*Simulation between 2008 and 2012*. The T-NET model obtained the best performance, with a mean RMSE of 1.6 °C *versus* 1.9 °C with the 0D model at the 128 stations (2008–2012) and improved simulations at 105 stations with a decrease of 0.4 °C in the RMSE compared with the 0D model (Figure 6a). Water temperature simulations were particularly improved by the T-NET model during winter (November– February) and summer (June–August) with a reducing of the RMSE by 0.7 °C compared with the 0D model, whatever the river size. The model performance is globally the same during spring and autumn.

For small rivers, the T-NET model generally performed considerably better than the 0D model, reducing mean daily RMSE over the year by more than 1 °C [Figure 6a (black dots) and d]. The 0D model did not take into account the downstream propagation of the thermal signal, and simulations were underestimated during winter and overestimated during summer (Figure 6d). The annual RMSE exceeded 2 °C at 38 stations, compared with only 20 with the T-NET model, which overcame these inaccuracies and reduced biases, especially in winter (−0.8 °C) and summer (−0.6 °C).

Performance at stations located on large rivers was similar with the two models, with a mean RMSE of 1.1 °C [Figure 6b (white dots) and c]. Far from the headwater, the memory of the upstream temperature is lost and weather is the main factor driving water temperature (Beaufort *et al.*, 2015), which explains the good performance of the 0D model for large rivers, similar to that of the T-NET model (Figure 6c). For stations close to the headwater, the weather

 

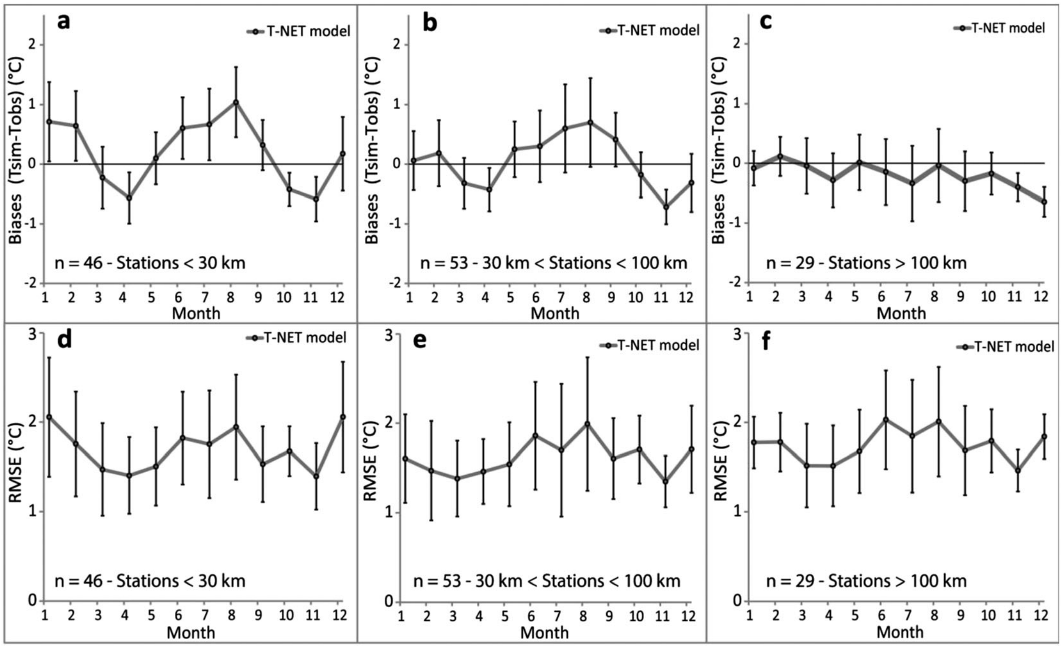


Figure 5. Biases and root mean square errors averaged over each month calculated with the T-NET model between 2008 and 2012 at daily time step at stations (a and d) less than 30 km; (b and e) between 30 and 100 km; and (c and f) more than 100 km from their headwater. Error bars represent 1 standard deviation of values

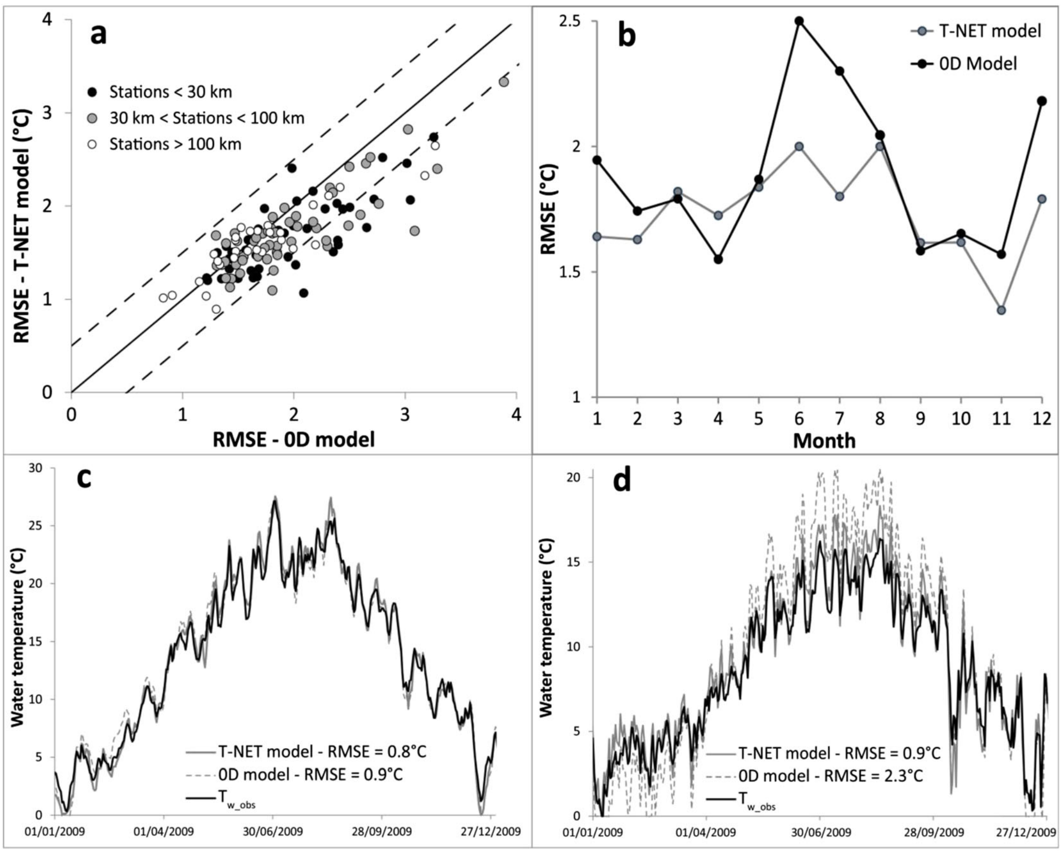


Figure 6. Performance of the T-NET and 0D models: (a) root mean square errors calculated at the 128 monitoring stations between 2008 and 2012 and (b) daily root mean square errors averaged over each month. Daily observed and simulated water temperatures by both models at two stations: (c) on a large river (drainage area = 38 300 km$^2$) and (d) on a small river (drainage area = 81 km$^2$)

effect is smaller, with greater influence of the headwater temperature, which may be colder (groundwater in summer, snowmelt) than the local water temperature determined by the 0D model. The T-NET model, which takes into account the propagation of the thermal signal from upstream to downstream, improved simulations, especially at stations on small and medium rivers that are more influenced by headwater conditions.

*Simulation during flood events in summer 1992 and winter 2003*. The largest summer flood of the Loire (between June and August) since 1984 occurred in 1992. Discharge at Dampierre (distance from headwater = 570 km) exceeded $1500\,\text{m}^3\,\text{s}^{-1}$ on 14th June, whereas the annual discharge at this point is $300\,\text{m}^3\,\text{s}^{-1}$ (1984–2012). During the flood between 5th June and 10th July, the temperature dropped by 3 °C at the Dampierre station. The mean daily biases calculated with the T-NET during the flood are 0.2 °C, while the mean biases calculated with the 0D model are 2.5 °C. The 0D model obtained a mean daily RMSE of 2.5 °C and failed to simulate the temperature decrease because by definition, this model only considers local forcing conditions (Figure 7a). The mean daily RMSE calculated with the T-NET model is 0.4 °C because this model takes into account the propagation of the thermal signal from upstream to downstream and showed excellent capacity to simulate the cooling of the river during the flood (Figure 7a). When the discharge rises rapidly, the flow velocity increases and the headwater temperature has more influence because the downstream travel time is shorter, slowing down the convergence of the stream temperature and the equilibrium temperature. During summer, the headwater temperature, considered as the groundwater temperature, is lower than the stream temperature by approximately 10 °C and has a buffering effect, leading to a drop in the stream temperature. In December 2003, the largest flood of the Loire since 1984 was observed, with discharge exceeding $3000\,\text{m}^3\,\text{s}^{-1}$ on 8th December (Figure 7b). The temperature observed at the Dampierre station decreased by more than 2 °C during the flood. The T-NET model reproduced this decrease well with a mean daily bias of 0.2 °C, while the 0D model overestimated the water temperature by 1 °C because it did not take into account the influence of upstream rivers. The T-NET simulated the cooling effect of the flood very accurately.

*Simulation of the hot summer of 2003 and the cold summer of 2002*. The summer of 2003 was marked by a severe drought (1 in 50 years; rainfall below 10 mm in August 2003 in the plain area) and a hot spell (maximum daily $T_a > 39$ °C in August 2003 and mean $T_a$ in August = 30 °C), with an increase of 3.2 °C in the mean summer air temperature compared with the 1974–2006 summer mean (Bustillo *et al.,* 2014; Moatar and Gailhard, 2006). This was an exceptional year because climate projections for the 21st century indicate increasing occurrences of hot and dry conditions compared with 2003 (Moatar *et al.,* 2010). Water temperatures simulated by the T-NET model for August 2003 were 0.5 °C colder than those simulated by the 0D model on average for all rivers located in the Loire basin. The difference of temperature simulated between both models could exceed 2 °C for rivers close to their headwater (Figure 8). These cold water streams are located in the upstream mountainous area of the basin where the air is colder (mean air temperature in August 2003 = 20 °C), and also in the middle sedimentary reaches of the basin where streams benefit more from groundwater supplies ($T_w < 14$ °C; dark blue Figure 8a) (Beaufort *et al.,* 2015). Temperatures simulated by the 0D model were influenced more by weather conditions, which led to a slightly higher simulated temperature in the lowland (85% of $T_w > 25$ °C with 0D

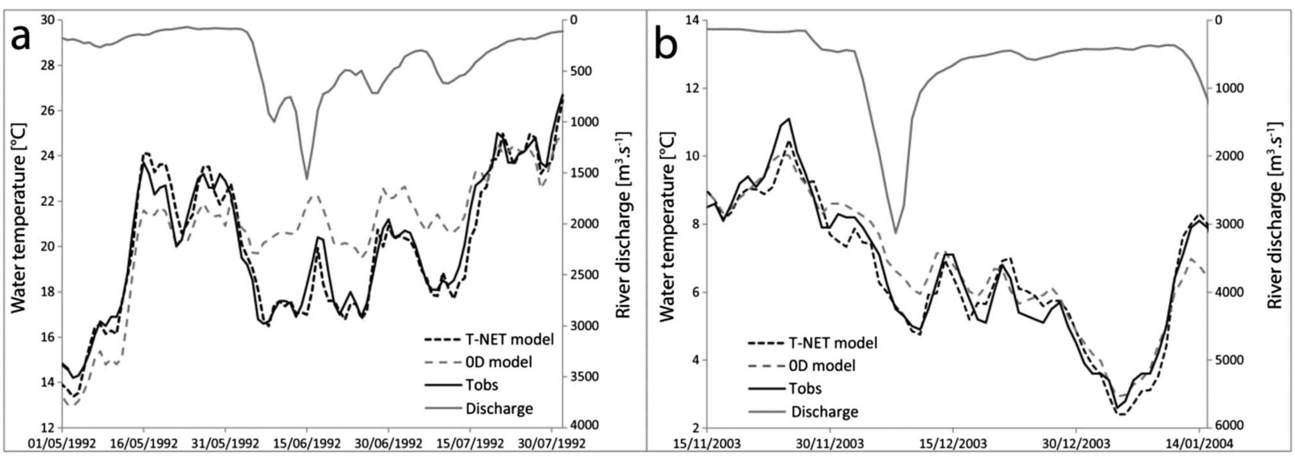


Figure 7. Water temperature of the Loire at Dampierre observed and simulated by the T-NET model and the 0D model during (a) the summer flood in June 1992 and (b) the winter flood in December 2003. The second axis represents the discharge simulated by the EROS hydrological model

 

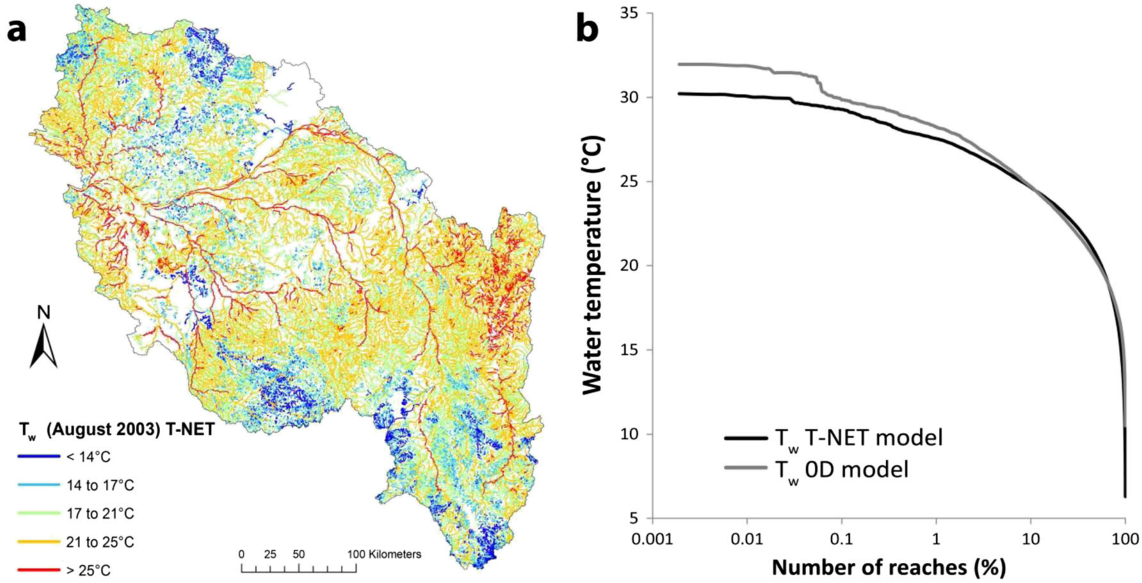


Figure 8. Water temperature simulated by (a) the T-NET model and (b) the 0D model in the Loire basin during the heat wave of August 2003

model *vs* 80% with T-NET model). Simulations on the Loire River and its main tributaries were similar with a temperature higher than 25 °C.

The summer of 2002 was colder than 2003 (maximum daily $T_a < 28$ °C in August 2002 and mean $T_a$ in August 23 °C). The performance of the two models for summer 2002 was similar, with a median RMSE of 1.7 °C obtained by the T-NET model and 1.8 °C by the 0D model (Figure 9a). However, the T-NET model performed better for the summer of 2003, with an RMSE lower than 1.5 °C at 49% of stations *versus* 28% with the 0D model (Figure 9b). RMSE was higher than 3 °C at 18% of stations with the 0D model *versus* 3% of stations with the T-NET model. Beaufort *et al.* (2015) showed that poorly simulated stations were largely fed by groundwater inputs, which maintained a relatively cool temperature over the entire period under study. The model failed to simulate this particularity and underestimated the cooling effect of groundwater, which had a stronger influence during the heat wave of 2003, especially on small streams. Conversely, the T-NET model was more efficient by taking the upstream influence into account, which improved simulations at small and medium rivers close to their headwater. The T-NET model is better at simulating the contrasting response of the thermal regime of streams during hot spells and can offer a better way of studying the thermal response of rivers to climate change than the 0D model.

### *Sensitivity analysis of input data*

Several input data, including river depth ($D$), groundwater flow ($Q_g$), shading factor (SF), headwater temperature ($T_{w\_head}$), river width ($B$), river discharge ($Q$) and flow velocity ($U$) remained difficult to quantify at the

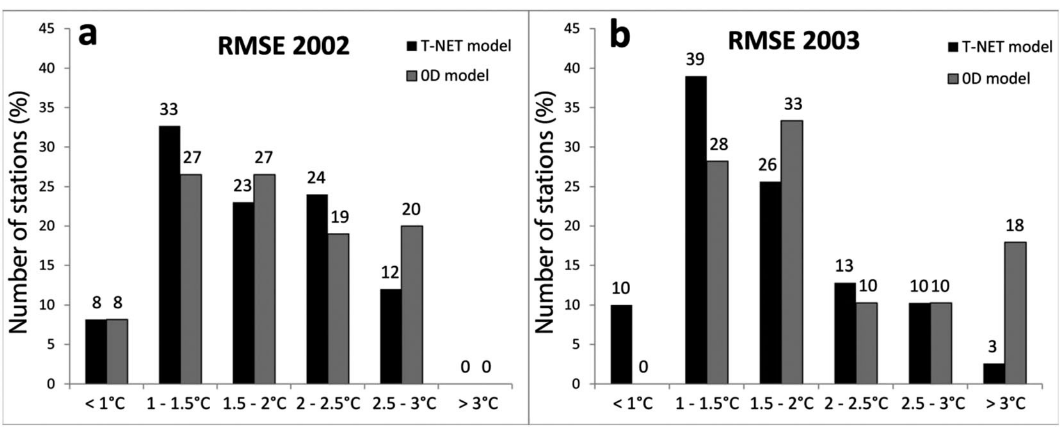


Figure 9. Root mean square errors calculated with the two models at the 47 stations available in (a) summer 2002 and (b) summer 2003 at a daily time

scale of a large regional watershed. To overcome these difficulties, we used a hydrological model to simulate the daily discharge at 368 subwatershed outlets and empirical formulae for stream morphological and hydraulic variables as described in the first section of this paper. Here, we will examine the influence of these data on water temperature simulations at the 128 monitoring stations.

Two types of controlling factor can be distinguished: factors influencing the mean water temperature and those influencing the water temperature variability.

In the first category, we could identify the SF, headwater temperature ($T_{w\_head}$) and the groundwater flow ($Q_g$). The SF had the most influence on the mean water temperature. At the 128 stations, a 50% variation in SF changed the annual water temperature by ±1.1 °C (Figures 10a and 11b). The major influence of SF occurred in summer where a variation of ±50% led to mean temperature changes higher than 1.5 °C. Narrow reaches (distance from headwater < 30 km) were more sensitive to SF changes (±2 °C) because the canopy shaded the whole reach area. Conversely, the presence of canopy along large rivers, such as the Loire (mean width = 500 m), changed the temperature by less than 0.1 °C. The SF is currently considered as constant throughout the year, which could explain the seasonality of biases for small and medium rivers in relation with the variation of the solar radiation. One way of improving this would be to take an SF variable governed by several parameters (vegetation cover, canopy height, position of the sun, river width and season). Recent studies have shown the importance of considering the shading variable because this factor can have a strong influence on the mean temperature (Moore *et al.,* 2014; Garner *et al.,* 2014).

A ±50% variation of the headwater temperature ($T_{w\_head}$) leads to a 0.5 °C change in the annual water temperature. The influence of $T_{w\_head}$ was greater in winter when the mean temperature changes exceed 0.8 °C on average, while changes are close to 0 in summer (Figure 10a). The propagation time was shorter in winter and slowed down the speed at which the stream temperature converges with the equilibrium temperature (Equation 2). In this case, $T_{w\_head}$ plays a major role in simulations and may impact the temperature, even 900 km downstream (±0.3 °C on the Loire River). Conversely, the influence of $T_{w\_head}$ in summer was very limited after 100 km, and $T_w$ was controlled by weather and local conditions, which explained the good performance of the 0D model for large rivers. Stations located on small rivers close to the headwater were the most affected by a change in $T_{w\_head}$ (±1.2 °C), showing the importance of determining the boundary conditions accurately ($T_{w\_head}$). While the estimation of $T_{w\_head}$ was good (see Section on Datasets), it could be expected that it would also be influenced by snowmelt and rainfall. These two factors are not currently included in the model, suggesting a possible line for improvement.

Groundwater flow [$m^3 s^{-1}$] was included in the streambed input equation to compute the heat budget. It had a buffering effect on the thermal regime of rivers, and a 50% increase could reduce the daily variation of water temperature by 0.3 °C (Figure 11b). The largest temperature changes occur at stations located in the central area of the basin composed of sedimentary rocks, which have a larger groundwater supply. At these stations, the mean water temperature could rise by 1.1 °C during winter and fall by 1 °C in summer with a groundwater input increase of 50% (Figure 11b).

In the second category of controlling factors, river discharge was the main factor influencing the water temperature variability. Discharge is used to calculate flow velocity and was a part of Equation 4 to determine the water temperature. Discharge has a strong influence on the daily water temperature variability and is a driver of the thermal inertia of the system. A 50% increase in the

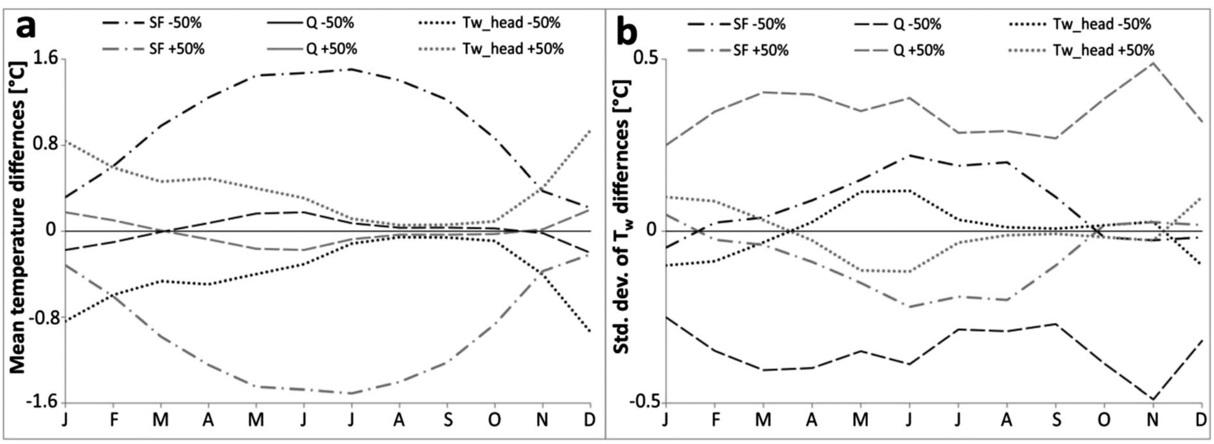


Figure 10. Model sensitivity evaluated at the 128 stations in 2008–2012: (a) distribution of mean river temperature differences and (b) water temperature variability with changes in shading factor (SF), headwater temperature ($T_{w\_head}$) and river discharge ($Q$)

 

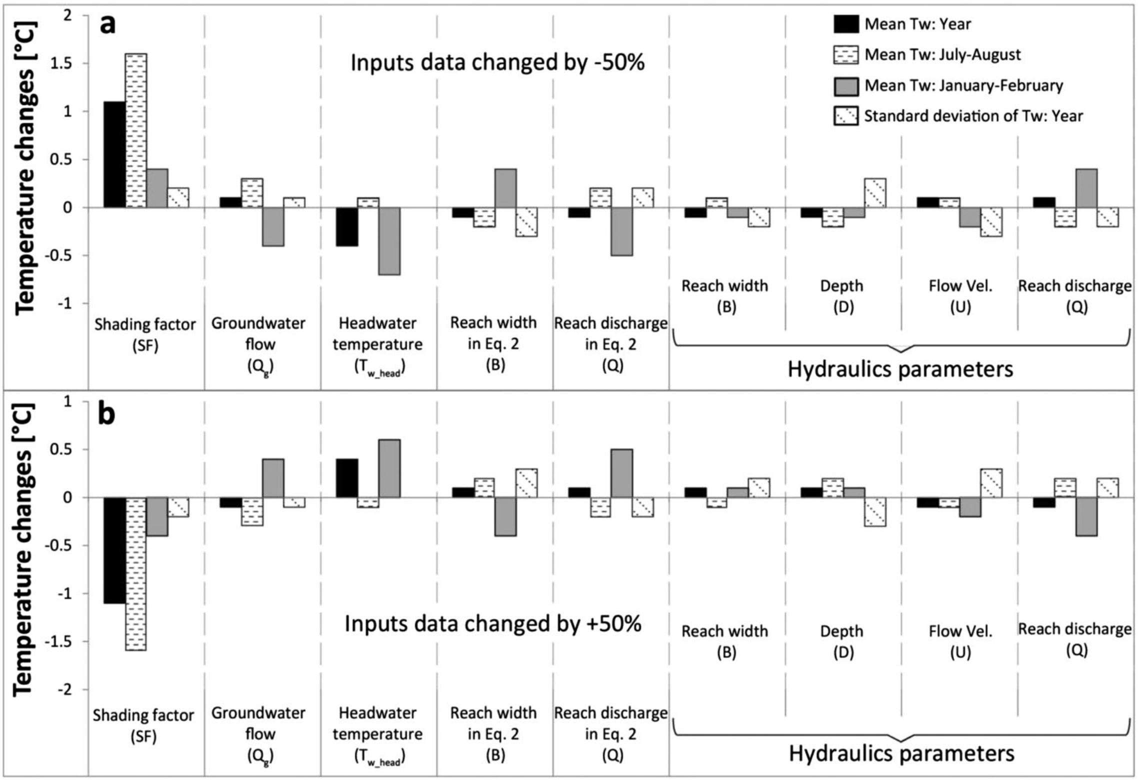


Figure 11. Model sensitivity: Distribution of mean river temperature differences and water temperature variability with changes in river depth, groundwater flow, shading factor, boundary conditions, river width, river discharge and flow velocity of (a) −50% and (b) +50% calculated at the 128 stations in 2008–2012

discharge led to a 0.3 °C rise in the daily water temperature amplitude (Figure 10b) and had more influence in winter at stations on large rivers (+0.5 °C). Conversely, a decrease in the discharge led to a reduction in the thermal inertia and a 0.3 °C drop in daily temperature amplitude (Figure 10b). River width was also included in Equation 2 and determined the exchange area between the river, the atmosphere and the groundwater. The water temperature tends to converge more quickly to the equilibrium temperature ($T_e$) if the river is very wide and the daily temperature variability is high (Figure 11). While the simulation of the discharge and the calculation of river width and river depth seem to be good (see Section on Datasets), we had few validation measures and some rivers could be poorly simulated. The manner in which the discharge is distributed within a subwatershed masks the specific hydrological behaviour of some rivers and could explain the poor simulation of local water temperature. One way of improving the simulation of river temperature would be to combine the T-NET model with a hydrological model in order to simulate the discharge in each stream.

## CONCLUSION

A key issue of this study concerns the improved performance of thermal simulations by applying the upstream–downstream propagation of the thermal signal at a regional scale (110 000 km$^2$). The performance level with the T-NET model improved at 105 stations, with a 0.4 °C decrease in the RMSE compared with the 0D model. Simulations at stations on small and medium rivers that are more influenced by headwater conditions were greatly improved, with a decrease of more than 1 °C in the mean RMSE. The T-NET appears to be considerably better than the 0D model at simulating specific events like the floods of June 1992 and the response of the thermal regime of streams during the heatwave of August 2003. Simulation of the downstream propagation of the thermal signal with the T-NET had a mean RMSE of 1.7 °C in summer 2003 *versus* 2.2 °C with the 0D model.

The sensitivity analysis identified the SF and the headwater temperature as the most influential factors on the simulated mean water temperature. This factor could be determined more accurately by taking into account a variable SF governed by several parameters (vegetation cover, canopy height, sun position, river width and season), which could lead to improved simulations of small and medium rivers. Another issue raised by this study is the strong influence of the headwater temperature calculated at the upstream boundary during winter and autumn. Several simulations were tested on the Loire, and water temperature can differ by more than 0.5 °C 900 km downstream. Conversely, the upstream conditions are more negligible in summer, particularly 100 km from the headwater, which explains the good performance of the 0D model on large rivers during summer (Beaufort *et al.,* 2015). Yearsley (2012) has shown the difficulty of simulating the correct temperature at the upstream boundary and its impact on simulations further downstream. There is a lack of validation data concerning the measurement of temperature at the upstream boundary, and to our knowledge, the temperature of the headwater at the scale of the Loire basin is not monitored, and it was therefore not possible to validate. This difficulty could be overcome if we had a representative sampling of temperature in the headwaters. The installation of a distributed temperature sensing system with an optic fibre cable along the first kilometres from the headwater could help to better estimate the longitudinal gradient of the stream temperature in the upper reaches (Westhoff *et al.,* 2007). The river discharge is the main factor influencing the water temperature variability. One way of improving the thermal simulation of river temperature would be to combine the T-NET model with a hydrological model in order to simulate the discharge in each stream at a higher temporal resolution.

Finally, this model by propagation offers a good compromise between performance and transferability. It can be easily transposed to changing forcing conditions (physically based structure) in any other catchment. Thermal simulations performed at a daily time step are spatially very consistent at the scale of a hydrographical reach (~1.7 km). The error structure was convincingly interpreted, and based on these results, a regionalized simulation of the impact of climate change on the thermal regime of rivers could be achieved.

## ACKNOWLEDGEMENTS

This work was realized in the course of work for a thesis funded by the Office National de l'Eau et des Milieux Aquatiques (ONEMA, National sponsor ID : 180068017 01720). It also benefitted from financial supports by the Fonds Européen de développement Régional (FEDER, European founds), the Etablissement Public Loire (EPL) and the water Agency of Loire Bretagne (AELB). Thanks are due to Meteo-France for the SAFRAN database, to EDF for the water temperature data at the station of Dampierre and to Valette *et al.* for the vegetation database from IRSTEA. We also thank Yann Jullian and the CaSciModOT federation (Calcul Scientifique et Modélisation Orléans Tours) for their assistance for the implementation of the model and for the calculations parallelization.

## REFERENCES

Beaufort A, Moatar F, Curie F, Ducharne A, Bustillo V, Thiéry D. 2015. River temperature modelling by Strahler order at the regional scale in the Loire River basin, France. *River Research and Applications, in press.* DOI:10.1002/rra.2888

Boyd M, Kasper B. 2003. Analytical methods for dynamic open channel heat and mass transfer: methodology for heat source model, version 7.0, Oregon Dept. of Env. Qual., Portland, Oreg.

Brutsaert W, Stricker H. 1979. An advection–aridity approach to estimate actual regional evapotranspiration. *Water Resources Research* **15**: 443–450.

Buisson L, Blanc L, Grenouillet G. 2008. Modelling stream fish species distribution in a river network: the relative effects of temperature *versus* physical factors. *Ecology of Freshwater Fish* **17**(2): 244–257.

Buisson L, Grenouillet G. 2009. Contrasted impacts of climate change on stream fish assemblages along an environmental gradient. *Diversity and Distributions* **15**(4): 613–626.

Bustillo V, Moatar F, Ducharne A, Thiéry D, Poirel A. 2014. A multimodel comparison for assessing water temperatures under changing climate conditions via the equilibrium temperature concept: case study of the Middle Loire River, France. *Hydrological Processes* **28**: 1507–1524. DOI:10.1002/hyp.9683

Caissie D. 2006. The thermal regime of rivers: a review. *Freshwater Biology* **51**: 1389–1406.

Carrivick JL, Brown LE, Hannah DM, Turner AGD. 2012. Numerical modelling of spatio-temporal thermal heterogeneity in a complex river system. *Journal of Hydrology* **414–415**: 491–502.

Chapra SC, Pelletier GJ, Tao H. 2008. QUAL2K: a modeling framework for simulating river and stream water quality, version 2.11: documentation and users manual, 109 pp., Civil and Environmental Engineering Dept., Tufts Univ., Medford, Mass.

Cole TM, Wells SA. 2002. CE-QUAL-W2: a two-dimensional, laterally averaged, hydrodynamic and water quality model, version 3.1, U.S.. Army Corps of Engineers Instruction Rep. EL-02-4, 131, pp. + Appendices, U.S. Army Corps of Engineers, Vicksburg, Miss.

Cox MM, Bolte JP. 2007. A spatially explicit network-based model for estimating stream temperature distribution. *Environmental Modelling & Software* **22**: 502–514.

Domisch S, Araujo MB, Bonada N, Pauls SU, Jahnig SC, Haase P. 2013. Modelling distribution in European stream macroinvertebrates under future climates. *Global Change Biology* **19**: 752–762. DOI:10.1111/gcb.12107

Edinger JE, Duttweiller D, Geyer J. 1968. The response of water temperatures to meteorological conditions. *Water Resources Research* **4**: 1137–1143.

Edinger JE, Brady DK, Geyer JC. 1974. Heat exchange and transport in the environment, in Cooling water discharge project (RP- 49), Rep. In *14, Electr.* Palo Alto, Calif: Power Res. Inst..

Garner G, Hannah DM, Sadler JP, *et al.* 2013. *River temperature regimes of England and* Wales: spatial patterns, inter-annual variability and climatic sensitivity. Hydrological Processes. doi: 10.1002/hyp.9992.

Garner G, Malcolm IA, Sadler JP, Hannah DM. 2014. What causes cooling water temperature gradients in forested stream reaches? *Hydrology and Earth System Sciences Discussions* **11**: 6441–6472. DOI:10.5194/hessd-11-6441-2014

Hannah DM, Garner G. 2015. River water temperature in the United Kingdom: changes over the 20th century and possible changes over the 21st century. *Progress in Physical Geography* **38**: 68–92. DOI:10.1177/0309133314550669

Herb WR, Stefan HG. 2011. Modified equilibrium temperature models for cold-water streams. *Water Resources Research* **47**: W06519. DOI:10.1029/2010WR009586

Kelleher C, Wagener T, Gooseff M, *et al.* 2012. Investigating controls on the thermal sensitivity of Pennsylvania streams. *Hydrological Processes* **27**: 771–785.

Lamouroux N, Pella H, Vanderbecq A, Sauquet E, Lejot J. 2010. Estimkart 2.0: Une plate-forme de modèles écohydrologiques pour contribuer à la gestion des cours d'eau à l'échelle des bassins français. Version provisoire. Cemagref – Agence de l'Eau Rhône-Méditerranée-Corse – Onema210.

Lassalle G, Rochard E. 2009. Impact of twenty-first century climate change on diadromous fish spread over Europe, North Africa and the Middle East. *Global Chang Biol* **15**: 1072–89.

Loinaz MC, Davidsen HK, Butts M, Bauer-Gottwein P. 2013. Integrated flow and temperature modeling at the catchment scale. *Journal of Hydrology* **495**: 238–251.

 

Moatar F, Gailhard J. 2006. Water temperature behaviour in the River Loire since 1976 and 1881. C.R. *Geosciences* **338**: 319–328.

Moatar F, Ducharne A, Thiéry D, Bustillo V, Sauquet E, Vidal JP. 2010. La Loire à l'épreuve du changement climatique. *Geosciences* **12**: 78–87. http://www.brgm.fr/dcenewsFile?ID=1306

Mohseni O, Stefan HG. 1999. Stream temperature/air temperature relationship: a physical interpretation. *Journal of Hydrology* **218**: 128–141.

Moore RD, Spittlehouse DL, Story A. 2005. Riparian microclimate and stream temperature response to forest harvesting: a review. *Journal of the American Water Resources Association* **41**(4): 813–834.

Moore RD, Leach JA, Knudson JM. 2014. Geometric calculation of view factors for stream surface radiation modelling in the presence of riparian forest. *Hydrological Processes* **28**: 2975–2986. DOI:10.1002/hyp.9848

O'Driscoll MA, DeWalle DR. 2006. Stream-air temperature relations to classify stream-ground water interactions in a karst setting, central Pennsylvania, USA. *Journal of Hydrology* **329**: 140–153.

Ouellet V, Secretan Y, St-Hilaire A, Morin J. 2014. Daily averaged 2D water temperature model for the St. Lawrence River. *River Research and Applications* **30**: 733–744. DOI:10.1002/rra.2664

Quintana-Seguí P, Le Moigne P, Durand Y, Martin E, Habets F, Baillon M, Canellas C, Franchisteguy L, Morel S. 2008. Analysis of near surface atmospheric variables: validation of the SAFRAN analysis over France. *J. App. Met. Clim.* **47**: 92–107. DOI:10.1175/2007JAMC1636.1

Sharma S, Jackson DA, Minns CK, Shuter BJ. 2007. Will northern fish populations be in hot water because of climate change? *Global Change Biology* **13**: 2052–2064. DOI:10.1111/j.1365-2486.2007.01426.x

Sridhar V, Sansone AL, LaMarche J, Dubin T, Lettenmaier DP. 2004. Prediction of stream temperature in forested watersheds. *Journal of the American Water Resources Association* **40**: 197–211.

Sun N, Yearsley J, Voisin N, Lettenmaier DP. 2014. A spatially distributed model for the assessment of land use impacts on stream temperature in small urban watersheds. *Hydrological Processes* DOI:10.1002/hyp.10363

Thiéry D. 1988. Forecast of changes in piezometric levels by a lumped hydrological model. *Journal of Hydrology* **97**: 129–148.

Thiéry D, Moutzopoulos C. 1995. Un modèle hydrologique spatialisé pour la simulation de très grands bassins: le modèle EROS formé de grappes de modèles globaux élémentaires. In *VIIIèmes journées hydrologiques de l'ORSTOM "Régionalisation en hydrologie, application au développement"*, Le Barbé et E (ed). ORSTOM Editions: Servat; 285–295.

Tisseuil C, Vrac M, Grenouillet G, Wade AJ, Gevrey M, Oberdorff T, Grodwohl JB, Lek S. 2012. Strengthening the link between climate, hydrological and species distribution modeling to assess the impacts of climate change on freshwater biodiversity. *Science of the Total Environment* **424**: 193–201.

Todd DK. 1980. *Groundwater Hydrology*. John Wiley: Hoboken, N. J.

Valette L, Piffady J, Chandesris A, Souchon Y. 2012. SYRAH-CE: description des données et modélisation du risque d'altération de l'hydromorphologie des cours d'eau pour l'Etat des lieux DCE. *Rapport final, Pôle Hydroécologie des cours d'eau Onema-Irstea Lyon, MALY-LHQ, juillet* **2012**: 104.

van Vliet MTH, Yearsley JR, Franssen WHP, Ludwig F, Haddeland I, Lettenmaier DP, Kabat P. 2012. Coupled daily streamflow and water temperature modelling in large river basins. *Hydrology and Earth System Sciences* **16**: 4303–4321.

Vidal JP, Martin É, Baillon M, Franchistéguy L, Soubeyroux JM. 2010. A 50-year high-resolution atmospheric reanalysis over France with the Safran system. *International Journal of Climatology* **30**(11): 1627–1644. DOI:10.1002/joc.2003

Westhoff MC, Savenije HHG, Luxemburg WMJ, Stelling GS, van de Giesen NC, Selker JS, Pfister L, Uhlenbrook S. 2007. A distributed stream temperature model using high resolution temperature observations. *Hydrology and Earth System Sciences* **11**: 1469–1480.

Yearsley JR. 2009. A semi-Lagrangian water temperature model for advection-dominated river systems. *Water Resources Research* **45**: W12405 DOI:10.1029/2008WR007629.

Yearsley JR. 2012. A grid-based approach for simulating stream temperature. *Water Resources Research* **48**: W03506.

 